Desalination and Water Treatment
www.deswater.com

doi: 10.1080/19443994.2015.1133325

57 (2016) 22370–22377
October

Taylor & Francis
Taylor & Francis Group

Influence of preparation method on the physicochemical properties and catalytic activity of SiO_2–TiO_2 mixed oxides

Robab Mohammadi

Department of Chemistry, Payame Noor University, P.O. Box 19395-3697, Tehran, Iran, Tel. +98 41 35412117; Fax: +98 41 35413381; email: mohammadi_rb@yahoo.com

Received 5 June 2015; Accepted 4 December 2015

ABSTRACT

In this study, SiO_2–TiO_2 mixed oxides with different physicochemical properties and various activities were prepared by sol–gel method under acid-catalyzed and base-catalyzed conditions. X-ray diffraction (XRD), scanning electron microscope, and energy dispersive X-ray spectroscopy (EDX) analysis methods were used for the characterization of prepared samples. The photocatalytic activity was evaluated vs. the decolorization of methyl orange (MO) under black-light radiation. The influence of synthesis method on the physicochemical properties such as crystalline structure, crystal size, morphology, and photocatalytic activity of samples was investigated. The XRD patterns showed that the sample prepared by sol–gel method under acid-catalyzed conditions has pure anatase phase, whereas the sample prepared by sol–gel method under base-catalyzed conditions has anatase-rutile mixed phase. SiO_2–TiO_2 mixed oxides prepared under acid-catalyzed conditions showed higher photoactivity in comparison with SiO_2–TiO_2 mixed oxides prepared under base-catalyzed conditions for the sake of reducing the crystallite size and agglomerations. The figures-of-merit based on electric energy consumption (electrical energy per order (E_{EO})) were evaluated in the photodecolorization of MO in the presence of prepared samples. The results showed that less energy is consumed during the decolorization of MO in the presence of SiO_2–TiO_2 mixed oxides prepared by sol–gel method under acid-catalyzed conditions.

Keywords: SiO_2–TiO_2 mixed oxides; Acid-catalyzed conditions; Physicochemical properties; Photocatalytic activity

1. Introduction

Heterogeneous photocatalytic degradation of water pollutants is one of the most promising techniques for waste management, particularly for degradation of organic pollutants [1]. Among the metal-oxide semiconductors suitable for photocatalytic degradation of environmental contaminants, titanium dioxide is the most widely applied catalyst, because of its fascinating physicochemical properties, high photoactivity, photocorrosion stability, nontoxic, and low cost [2]. The available surface area of TiO_2 can be enhanced by the addition of silica [3]. Therefore, adsorption of pollutant molecules on the surface of SiO_2 is increased, so the photoactivity of TiO_2 is improved [4]. Also, the addition of silica enhances the content of surface-adsorbed water and hydroxyl groups affects the photocatalytic activity of SiO_2–TiO_2 mixed oxides [5,6]. Ingale and his co-workers demonstrated that SiO_2–TiO_2 nano-composite aerogel has great potential to use as photocatalyst for oxidation of trinitrotoluene (TNT)

[3]. Properties of SiO_2–TiO_2 mixed oxides can be strongly influenced by the preparation method [7]. Silica–titania mixed oxides have been synthesized via different methods such as chemical vapor deposition (CVD), sol–gel, hydrothermal, micro emulsion [8–10], microwave, and ultrasonic micro emulsion. Among these techniques, the sol–gel method is the most popular method, due to the purity of oxides obtained, low price, better control over stoichiometric composition, better homogeneity, and the lower synthesis temperatures [11–13].

Although there are a variety of reports on synthesis of SiO_2–TiO_2 mixed oxides, however, a comparative research to emphasize the effect of the various preparation methods on the physicochemical properties and activity of SiO_2–TiO_2 mixed oxides has not been yet reported. Herein, we report the synthesis of SiO_2–TiO_2 mixed oxides by sol–gel method under acid-catalyzed and base-catalyzed conditions. The purpose of this work is to investigate the relationship between physicochemical properties, photoactivity, and preparation method. Also, electrical energy consumption and treatment cost are calculated during MO decolorization because the most important parameter in selecting a waste treatment technology is economics.

2. Materials and methods

2.1. Materials

Tetraethyl orthosilicate (TEOS), Titanium n-butoxide (TBOT), isopropanol, ethanol, sodium hydroxide, and nitric acid were prepared from Merck chemical company and used without further purification. Methyl orange (MO) was used as a model pollutant to measure the photocatalytic activity of synthesized samples.

2.2. Sample preparation

2.2.1. Preparation of SiO_2–TiO_2 mixed oxides by sol–gel method under acid-catalyzed conditions

SiO_2–TiO_2 mixed oxides with various SiO_2 contents were prepared, and the photocatalytic performance was evaluated to select the optimum SiO_2 content. Initially, TBOT was slowly dissolved in absolute ethanol. Then, distilled H_2O was added drop by drop into a flask containing TBOT/EtOH mixture under reflux and magnetic stirring. The molar ratio of TBOT/EtOH/H_2O was 1:1:65. The yellowish transparent titania sol was yielded after continuously stirring for 3 h. TEOS was dissolved in ethanol, after which a few drops of nitric acid were added to TEOS as catalyst. The pH of mixed solution was adjusted to about 3. The molar ratio of TEOS/EtOH was 1:2. Afterward, the mixture was kept in a water bath maintained at 70˚C for 2 h. This mixture was added drop wise to the titania sol and stirred for 1 h at reflux temperature. This solution was placed in a Teflon-lined stainless steel autoclave, in which it was heated at 150˚C for 24 h, and then calcined at 500˚C for 2 h with a heating rate of 10˚C/min in air atmosphere. In order to detect the optimum content of SiO_2, several samples were prepared by changing the SiO_2 content from 0 to 20 mol%. The best photocatalyst procured in these conditions was designated as TS_{HNO_3}.

2.2.2. Preparation of SiO_2–TiO_2 mixed oxides by sol–gel method under base-catalyzed conditions

After detection of the optimum content of SiO_2, SiO_2–TiO_2 mixed oxides were synthesized with the same optimum content of SiO_2 by sol–gel method under base-catalyzed conditions as follows.

A mixture of distilled H_2O and isopropanol was added drop by drop into a flask containing TBOT and isopropanol. The mixture was aged for 3 h under continuous stirring at room temperature. The molar ratio of TBOT/iso-PrOH/H_2O was 1:29:19. TEOS was dissolved in isopropanol, after which a few drops of nitric acid were added to TEOS as catalyst. Afterward, the mixture was kept in a water bath maintained at 70˚C for 2 h. TEOS and TBOT precursors were then mixed and stirred for 15 min. The pH value was adjusted by adding sodium hydroxide to about 9. The mixture was aged for 3 h under continuous stirring at room temperature. After standing at room temperature for 24 h, SiO_2–TiO_2 mixed oxides were obtained by calcining the obtained xerogel at 450˚C for 3 h and grinding. The catalyst procured by this method was designated as TS_{NaOH}.

2.3. Characterization of SiO_2–TiO_2 mixed oxides

The crystal phase composition and the crystallite size of TS_{HNO_3} and TS_{NaOH} were recorded using X-ray diffraction (XRD) (Siemens/D5000) with Cu Kα radiation (0.15478 nm) in the 2θ scan range of 10˚–70˚. The average crystallite size (D in nm) was calculated by Scherrer's equation [14]:

$$D = \frac{k\lambda}{\beta \cos \theta} \quad (1)$$

where k is a constant equal to 0.89, λ, the X-ray wavelength equal to 0.154056 nm, β, the full width at half

maximum intensity (FWHM) and θ, the half diffraction angle. The phase content of a sample can be calculated from the integrated intensities of anatase (I_A) and rutile (I_R) peaks using the following formula [15]:

$$\text{Rutile phase}\,\% = \frac{100}{1 + 0.8\,\frac{I_A}{I_R}} \quad (2)$$

The texture and morphology of the prepared samples were measured by scanning electron microscope (SEM) (Philips XL-30ESM). The chemical composition of the prepared catalyst was analyzed by an energy dispersive X-ray spectroscopy (EDX) system.

2.4. Photocatalytic decolorization procedures

Photocatalytic decolorization of dye was conducted in a batch quartz reactor. All photocatalytic experiments were applied at ambient temperature and atmospheric pressure. Artificial illumination was provided by black light 36 W (UV-A) with a wavelength peak at 365 nm, which positioned above to the reactor. In each run, 400 mg L^{-1} SiO_2–TiO_2 mixed oxides and 20 mg L^{-1} MO were fed into the quartz tube reactor and placed in the dark condition for 30 min with continuous stirring for adsorption–desorption equilibrium and then exposed to black-light illumination. Every 3 min as interval time, a sample was withdrawn and centrifuged to remove catalyst particles, and the concentration of dye was detected by UV–vis Perkin-Elmer 550 SE spectrophotometer at wavelengths of 465 nm.

3. Results and discussion

3.1. Characterization of prepared samples

Fig. 1 shows XRD patterns of TS_{HNO_3} and TS_{NaOH}. The crystallite size of samples is calculated using the Scherrer's equation based on the full peak width at half maximum intensity (FWHM) of anatase (1 0 1) and rutile (1 1 0) phases. From Fig. 1(a), pure anatase phase was observed for TS_{HNO_3}. The average size of crystallites for TS_{HNO_3} determined from the XRD pattern based on the Scherrer's formula was 8 nm. However, the XRD results of TS_{NaOH} showed a phase distribution of 65:35 (percentage) anatase: rutile, with crystallite size of 22 nm for anatase and 18 nm for rutile (Fig. 1(b)). TS_{HNO_3} shows less crystallite size suggesting higher surface area available for catalysis. The rate at which hydrolysis and condensation reactions take place is important factors influencing the properties of the final product. Under acid-catalyzed conditions, the hydrolysis is favored, the condensation reactions are limiting. So, acid catalyzed gels are polymeric type with smaller particle size and high-surface area [16]. Under basic conditions, the hydrolysis and particle nucleation processes are rate determining and the condensation processes are dominant [17]. So, the molecules of precursors are aggregated to larger, and denser particles than at low pH. Therefore, base catalyzed gels are colloidal type and have bigger particle size with relatively less specific surface area. No SiO_2 crystal phase was observed in samples. This shows that SiO_2 existed as an amorphous phase in the SiO_2–TiO_2 mixed oxides [18].

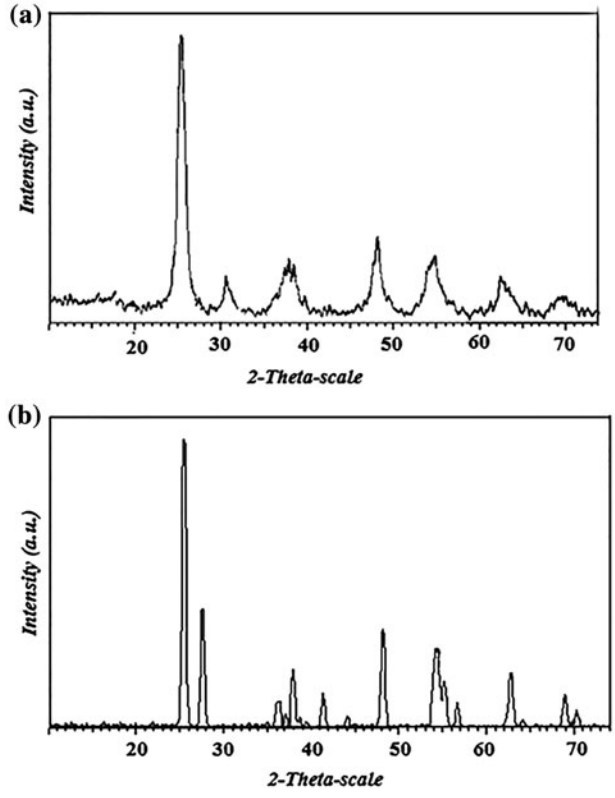

Fig. 1. XRD patterns of (a) TS_{HNO_3} and (b) TS_{NaOH}.

Fig. 2(a) shows SEM micrograph of TS_{HNO_3}. This image shows particles with good homogeneity, spherical morphology, and slight agglomeration. The SEM image of TS_{NaOH} is shown in Fig. 2(b). This image shows a dense structure with uniform particles which are coherent together. The structure of the metal oxide prepared via sol–gel method depends on the hydrolysis and condensation reactions which can be controlled by the solution's pH [19]. Under acid-catalyzed conditions, the hydrolysis kinetic is favored instead of the condensation. Under base-catalyzed conditions,

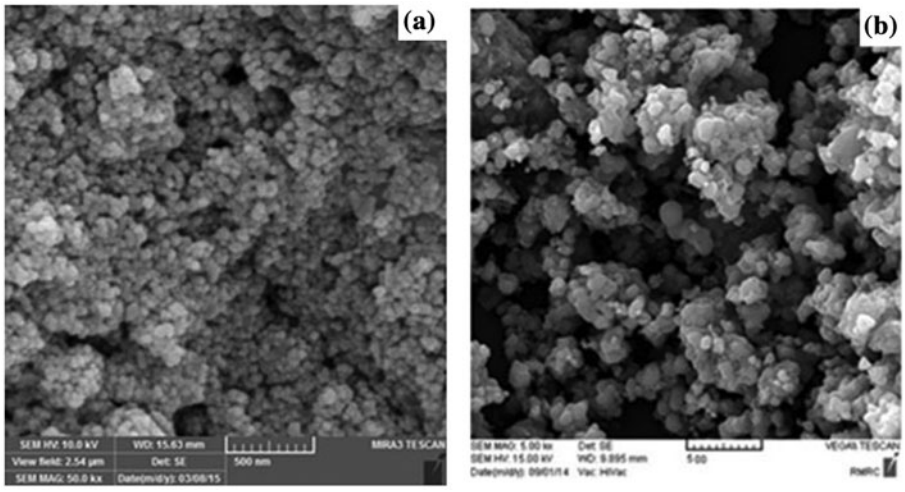

Fig. 2. SEM images of (a) TS_{HNO_3} and (b) TS_{NaOH}.

condensation is faster than hydrolysis, resulting in a highly condensed species that may agglomerate into fine particles [20]. Agglomeration of TS_{NaOH} is higher than that of TS_{HNO_3}. Since less particle agglomeration occurred for TS_{HNO_3}, the large surface area conveys high adsorption abilities of this catalyst.

Fig. 3 shows the EDX spectrum of TS_{HNO_3}. TiO_2 peaks can be seen at 0.5 and 4.5 keV which confirms the presence of titanium dioxide. SiO_2 peaks can be observed at 2.0 keV to confirm the presence of SiO_2.

3.2. Photocatalytic activity

The Langmuir–Hinshelwood (L–H) model has often been applied for the photodegradation kinetics of

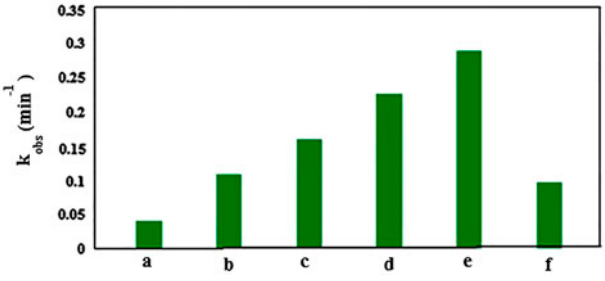

Fig. 4. Influence of SiO_2 content on the photocatalytic activity of SiO_2–TiO_2 mixed oxides prepared by sol–gel method under acid-catalyzed conditions: (a) Pure TiO_2, (b) 2 mol% SiO_2–TiO_2, (c) 5 mol% SiO_2–TiO_2, (d) 10 mol% SiO_2–TiO_2, (e) 15 mol% SiO_2–TiO_2, and (f) 20 mol% SiO_2–TiO_2.

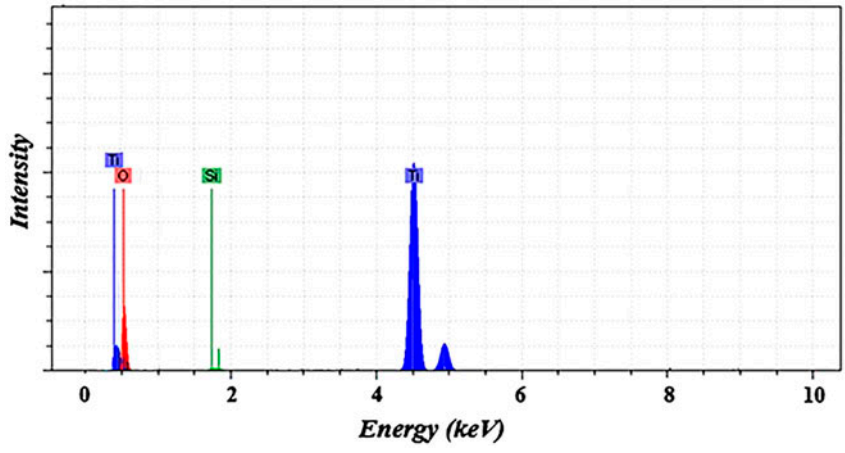

Fig. 3. EDX pattern of TS_{HNO_3}.

organic pollutants [21]. This model can cover properties of the compound on the photocatalyst surface as [22]:

$$-\frac{d[MO]}{dt} = \frac{k_{L-H}\, k_{ads}\, [MO]}{1 + k_{ads}\, [MO]} \quad (3)$$

where k_{L-H} is the reaction rate constant (mg L^{-1} min^{-1}), k_{ads} is the adsorption coefficient of pollutant on the photocatalyst (mg^{-1} L), and [MO] is the concentration of MO (mg L^{-1}). For low concentrations of MO (i.e. k_{ads} [MO] << 1), the L–H equation changes into a pseudo-first-order kinetics law as the following equation:

$$-\frac{d[MO]}{dt} = k_{obs}[MO] \quad (4)$$

where $k_{obs} = k_{L-H}\, k_{ads}$ is the pseudo-first-order rate constant. With integrating Eq. (4), we obtain:

$$\ln\frac{[MO]_0}{[MO]} = k_{obs}\, t \quad (5)$$

where $[MO]_0$ is the initial concentration of MO (mg L^{-1}). The semi-logarithmic graph of the concentration of MO in the presence of prepared samples vs. irradiation time yield straight lines, which confirms the pseudo-first-order kinetics. The pseudo-first-order reaction rate constant (k_{obs}) is chosen as the basic kinetic parameter to compare the photocatalytic activity of synthesized photocatalysts. The results of degradation of MO using SiO_2–TiO_2 mixed oxides with various SiO_2 contents prepared by the sol–gel method under acidic conditions are illustrated in Fig. 4. It could be observed that photocatalytic activity is increased with increasing content of SiO_2. When the content of SiO_2 enhances to 15 mol%, the photocatalytic activity of SiO_2–TiO_2 significantly increases. The acidity of the binary oxide is increased by adding SiO_2 in TiO_2. The increase in acidity has been explained via the model proposed by Guan [23]. According to this model, doped SiO_2 cation enters the lattice of TiO_2, and retains its original coordination number. The doped cation is still bonded to the same number of oxygen atoms despite coordination variations in the oxygen atoms, and so, a charge imbalance can be produced. However, the charge imbalance must be satisfied. Therefore, Lewis sites are formed because of the positive charge in the SiO_2–TiO_2. The surface with improved acidity adsorbs more OH radicals which led to enhance the photocatalytic activity and complete decolorization of MO. For too large contents of SiO_2, the surface active sites can be covered by inactive SiO_2 [24,25]. So, the photocatalytic activity of 20 mol% SiO_2–TiO_2 is decreased. Therefore, 15 mol% was selected as the optimum percentage of SiO_2 in SiO_2–TiO_2 mixed oxides and TS_{NaOH} was prepared with the same percentage of SiO_2.

The synthesis route of SiO_2–TiO_2 was assigned as an important parameter which can influence the efficiency of photocatalyst. From Fig. 5, the photocatalytic activity of TS_{HNO_3} is higher than that of TS_{NaOH}. Different parameters such as crystalline phase, crystalline size, and morphology of samples can affect the photoactivity of photocatalysts [26]. According to the XRD results, TS_{NaOH} is a combination of anatase (65%) and rutile (35%) phases. Whereas TS_{HNO_3} has pure anatase phase. It is known that anatase phase shows high activity in photocatalytic applications in comparison with rutile phase [27]. Particle size is an important parameter affecting photocatalytic activity since it directly impacts the specific surface area of a catalyst. When particle size is small, the number of active surface sites enhances as well as the surface charge carrier transfer rate in photocatalysis [28,29]. TS_{HNO_3} with small particle size can show high-photocatalytic activity. Particle agglomeration of TS_{HNO_3} is less than that of TS_{NaOH}. It can provide higher surface area for this sample. Large specific surface area can allow more pollutants to be absorbed onto the surface of catalyst [30]. Therefore, TS_{HNO_3} is a photocatalyst with better activity.

3.3. Spectral changes of MO during photodecolorization

Fig. 6 displays changes in the UV–vis absorption spectra of MO solution during the photocatalytic decolorization. The decrease in the absorption peak of MO at λ = 465 nm implies a rapid decolorization of pollutant [31]. Furthermore, this reduction is meaningful with respect to –N=N– bond of MO, as the most active site for oxidative attack [32]. The effect is related to a catalytic influence because no alteration in absorption was observed in the absence of SiO_2–TiO_2, even for large irradiation times. In the presence of

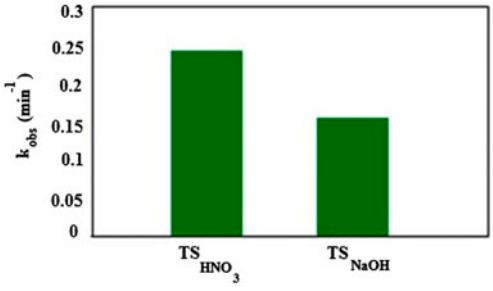

Fig. 5. Photocatalytic decolorization of MO in the presence of TS_{HNO_3} and TS_{NaOH}.

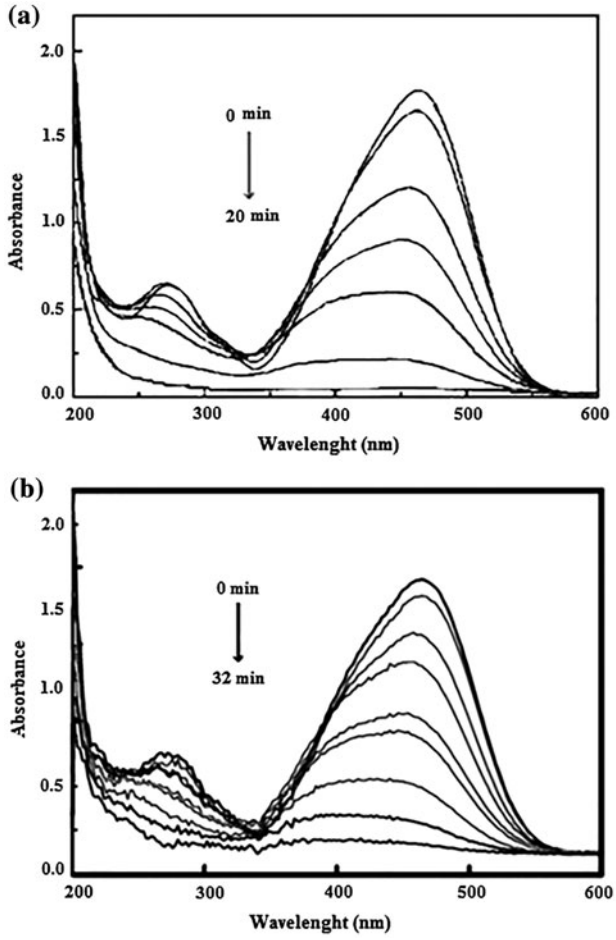

Fig. 6. Absorbance spectra of MO during the course of reaction catalyzed by (a) TS_{HNO_3} and (b) TS_{NaOH}.

TS_{HNO_3}, around 60% of decolorization was observed after 15 min illumination with black light (36 W) and the complete decolorization of the pollutant was reached at 20 min illumination. Before 15 min of irradiation, a slight decolorization was observed; this indicated that decolorization of the dye solution was mainly attributed to the adsorption of TS_{HNO_3} [33]. After 15 min of reaction, the decolorization rate was distinct because of the dye sensitization of the catalyst, which resulted from the adsorption of MO on TS_{HNO_3} [32]. Thus, the decolorization of MO by photocatalytic decolorization under black-light irradiation was accelerated thereafter. However, in the presence of TS_{NaOH}, complete decolorization of MO was observed after 32 min irradiation with black light.

3.4. Electrical energy efficiency

The evaluation of the treatment costs is one of the aspects that require more consideration. There are a number of important parameters in selecting a waste treatment process, including economics, economy of scale, regulations, effluent quality goals, operation (maintenance control, safety), and robustness (flexibility to change/upsets) [34]. Among these parameters, economics is often paramount. Since photocatalytic degradation process is electric energy intensive process, and electric energy can represent a major fraction of the operating costs, simple figures-of-merit based on electric energy consumption can be very helpful and informative [35]. The suitable figure-of-merit in the low pollutant concentration is the electrical energy per order (E_{E0}). E_{E0} (kWh/m^3/order) can be calculated from the following equations:

$$E_{E0} = \frac{P_{el} \times t \times 1{,}000}{V \times 60 \times \log\left(\frac{C_0}{C}\right)} \quad (6)$$

where P is the input power (kW) to the AOP system, t is the illumination time (min), V is the volume of water (L) in the reactor, C_0 and C are the initial and final MO concentrations, respectively [36]. This equation for a pseudo-first-order reaction in a batch reactor can be written as follow:

$$E_{E0} = \frac{P_{el} \times 38.4}{V \times k_{obs}} \quad (7)$$

where k_{obs} is the pseudo-first-order reaction rate constant (min^{-1}).

The E_{EO} amount for TS_{HNO_3} (22.374 kWh/m^3/order) is less than that of TS_{NaOH} (35.081 kWh/m^3/order). It is helpful to relate the values of electrical energy found in this work to the operation costs. By considering 0.036 US $ per kW per h as the cost of electricity in Iran, the contribution to operation costs of MO decolorization from electrical energy will be 0.805 and 1.262 US $ per m^3, for TS_{HNO_3}, and TS_{NaOH}, respectively. Thus, TS_{HNO_3} is more economical than TS_{NaOH}, due to decrease in energy required.

4. Conclusions

SiO_2–TiO_2 mixed oxides with different physicochemical properties and various photocatalytic activities were prepared via sol–gel method under acid-catalyzed and base-catalyzed conditions. The crystal structure, morphology, and photocatalytic activity were strongly influenced by preparation method. Results of photocatalytic activity indicated that SiO_2–TiO_2 mixed oxides prepared under acid-catalyzed conditions were more efficient than SiO_2–TiO_2 mixed oxides synthesized

under base-catalyzed conditions in the decolorization of MO from aqueous solution. Based on this research work, preparation method correlates with crystallinity, phase structure, morphology, and photocatalytic activity. The electrical energy consumption per order of magnitude for photodecolorization of MO was lower in the presence of TS_{HNO_3} than that of TS_{NaOH}. As technical advantages, this research provides an approach for highly efficient route to prepare highly active photocatalyst.

Acknowledgment

I express my gratitude to the Payame Noor University of Iran for supporting this project.

References

[1] A. Felix, A. Andrew, A. Mededode, Heterogeneous photocatalytic degradation of naphthalene using periwinkle shell ash: Effect of operating variables, kinetic and isotherm study, S. Afr. J. Chem. Eng. 19 (2014) 31–45.

[2] S. Bagheri, N. Muhd Julkapli, S. Bee Abd Hamid, Titanium dioxide as a catalyst support in heterogeneous catalysis, Sci. World. J. (2014) Article ID 727496 21. http://dx.doi.org/10.1155/2014/727496.

[3] S.V. Ingale, P.B. Wagh, A.K. Tripathi, A.S. Dudwadkar, S.S. Gamre, P.T. Rao, I.K. Singh, S.C. Gupta, Photo catalytic oxidation of TNT using TiO_2-SiO_2 nano-composite aerogel catalyst prepared using sol-gel process, J. Sol-Gel Sci. Technol. 58 (2011) 682–688.

[4] K.J.A. Raj, B. Viswanathan, Synthesis of nickel nanoparticles with fcc and hcp crystal structures, Ind. J. Chem. A. 59 (2011) 176–179.

[5] H. Chun, W. Yizhong, T. Hongxiao, Influence of adsorption on the photodegradation of various dyes using surface bond-conjugated TiO_2/SiO_2 photocatalyst, Appl. Catal. B: Environ. 35 (2001) 95–105.

[6] C. Xie, Z. Xu, Q. Yang, B. Xue, Y. Du, J. Zhang, Enhanced photocatalytic activity of titania–silica mixed oxide prepared via basic hydrolyzation, Mater. Sci. Eng. B 112 (2004) 34–41.

[7] K. Balachandran1, R. Venckatesh, R. Sivaraj, Photocatalytic decomposition of isoland black by TiO_2, TiO_2-SiO_2 core shell nanocomposites, Int. J. Res. Eng. Technol. 2 (2013) 46–51

[8] A. Feinle, F. Lavoie-Cardinal, J. Akbarzadeh, H. Peterlik, M. Adlung, C. Wickleder, N. Hüsing, Novel sol–gel precursors for thin mesoporous Eu^{3+}-doped silica coatings as efficient luminescent materials, Chem. Mater. 24 (2012) 3674–3683.

[9] A. Mahyar, M.A. Behnajady, N. Modirshahla, Characterization and photocatalytic activity of SiO_2–TiO_2 mixed oxide nanoparticles prepared by sol-gel method, Indian J. Chem. 49A (2010) 1593–1600.

[10] N. Venkatachalam, M. Palanichamy, V. Murugesan, Sol–gel preparation and characterization of nanosize TiO_2: Its photocatalytic performance, Mater. Chem. Phys. 104 (2007) 454–459.

[11] M. Farahmandjou, P. khalili, Morphology Study of anatase nano-TiO_2 for Self-cleaning Coating, Int. J. Fundam. Phys. Sci. 3 (2013) 54–56.

[12] N.N. Binitha, Z. Yaakob, R. Resmi, Influence of synthesis methods on zirconium doped titania photocatalysts, Cent. Eur. J. Chem. 8 (2010) 182–187.

[13] A.A. Aal, S.A. Mahmoud, A.K. Aboul-Gheit, Sol–gel and thermally evaporated nanostructured thin ZnO films for photocatalytic degradation of trichlorophenol, Nanoscale Res. Lett. 4 (2009) 627–634.

[14] M.R. Parra, F.Z. Haque, Aqueous chemical route synthesis and the effect of calcination temperature on the structural and optical properties of ZnO nanoparticles, J. Mater. Res. Technol. 3 (2014) 363–369.

[15] C. Shifu, Y. Xiaoling, L. Wei, Preparation and photocatalytic activity evaluation of composite photocatalyst Fe-TiO_2/TiO_2, ECS Trans. 21 (2009) 3–22.

[16] T. Matsoukas, E. Gulari, Dynamics of growth of silica particles from ammonia-catalyzed hydrolysis of tetraethyl-orthosilicate, J. Colloid Interface Sci. 124 (1988) 252–261.

[17] K. Sinkó, Influence of chemical conditions on the nanoporous structure of silicate aerogels, Materials 3 (2010) 704–740.

[18] T.M.L. Goerne, M.A.A. Lemus, V.A. Morales, E.G. Lopez, P.C. Ocampo, Study of bacterial sensitivity to Ag–TiO_2 nanoparticles, J. Nanomed. Nanotech. S5–003 (2012) 1–7, doi: 10.4172/2157-7439.S5-003.

[19] C. Chiang, C.M. Ma, D.L. Wu, H.C. Kuan, Preparation, characterization, and properties of novolac-type phenolic/SiO_2 hybrid organic-inorganic nanocomposite materials by sol-gel method, J. Polym. Sci. Part A: Polym. Chem. 41 (2003) 905–913.

[20] S. Vives, C. Meunier, Influence of the synthesis route on sol-gel SiO_2–TiO_2 (1:1) xerogels and powders, Ceram. Int. 34 (2008) 37–44.

[21] R. Mohammadi, M. Mohammadi, Photocatalytic removal of methyl orange using Ag/Zn–TiO_2 nanoparticles prepared by different methods, Desalin. Water Treat. (2015) 1–9, in press, doi: 10.1080/19443994.2015.1041160.

[22] C.S. Turchi, D.F. Ollis, Photocatalytic degradation of organic water contaminants: Mechanisms involving hydroxyl radical attack, J. Catal. 122 (1990) 178–192.

[23] K. Guan, Relationship between photocatalytic activity, hydrophilicity and self-cleaning effect of TiO_2/SiO_2 films, Surf. Coat. Technol. 191 (2005) 155–160.

[24] F. Sayilkan, M. Asilturk, S. Sener, S. Erdemoglu, M. Erdemoglu, H. Sayilkan, Hydrothermal synthesis, characterization and photocatalytic activity of nanosized TiO_2 based catalysts for Rhodamine B degradation, Turk. J. Chem. 31 (2007) 211–221.

[25] Y. Yao, D.W. Goodman, New insights into structure–activity relationships for propane hydrogenolysis over Ni–Cu bimetallic catalysts, RSC. Adv. 5 (2015) 43547–43551.

[26] M. Zhou, J. Yu, B. Cheng, Effects of Fe-doping on the photocatalytic activity of mesoporous TiO_2 powders prepared by an ultrasonic method, J. Hazard. Mater. 137 (2006) 1838–1847.

[27] B. Choudhury, A. Choudhury, Local structure modification and phase transformation of TiO_2 nanoparticles initiated by oxygen defects, grain size, and annealing temperature, Int. Nano. Lett. 3 (2013) 1–9.

[28] A. Primo, A. Corma, H. García, Titania supported gold nanoparticles as photocatalyst, Phys. Chem. Chem. Phys. 13 (2011) 886–910.
[29] X. Sun, H. Liu, J. Dong, J. Wei, Y. Zhang, Preparation and characterization of Ce/N-codoped TiO_2 particles for production of H_2 by photocatalytic splitting water under visible light, Catal. Lett. 135 (2010) 219–225.
[30] S. Chaturvedi, P.N. Dave, N.K. Shah, Applications of nano-catalyst in new era, J. Saudi Chem. Soc. 16 (2012) 307–325. Availbale from: <http://www.sciencedirect.com/science/article/pii/S1319610311000305-aff2>.
[31] R. Mohammadi, B. Massoumi, H. Eskandarloo, Preparation and characterization of Sn/Zn/TiO_2 photocatalyst for enhanced amoxicillin trihydrate degradation, Desalin. Water Treat. 53 (2015) 1995–2004.
[32] M.M. Khan, J. Lee, M.H. Cho, Au@TiO_2 nanocomposites for the catalytic degradation of methyl orange and methylene blue: An electron relay effect, J. Ind. Eng. Chem. 20 (2014) 1584–1590.
[33] C.C. Chen, Degradation pathways of ethyl violet by photocatalytic reaction with ZnO dispersions, J. Mol. Catal. A: Chem. 264 (2007) 82–92.
[34] H. Zhu, R. Jiang, Y. Fu, Y. Guan. J. Yao, L. Xiao, G. Zeng, Effective photocatalytic decolorization of methyl orange utilizing TiO_2/ZnO/chitosan nanocomposite films under simulated solar irradiation, Desalination 286 (2012) 41–48.
[35] N. Daneshvar, S. Aber, M.S. Seyed Dorraji, A.R. Khataee, M.H. Rasoulifard, Preparation and investigation of photocatalytic properties of ZnO nanocrystals: Effect of operational parameters and kinetic study, Int. J. Chem. Nucl. Mater. Metall. Eng. 1 (2007) 66–71.
[36] N. Daneshvar, A. Aleboyeh, A.R. Khataee, The evaluation of electrical energy per order (EEo) for photooxidative decolorization of four textile dye solutions by the kinetic model, Chemosphere 59 (2005) 761–767.